

# JOURNAL OF SCIENCE



SAKARYA UNIVERSITY

## Sakarya University Journal of Science

ISSN 1301-4048 | e-ISSN 2147-835X | Period Bimonthly | Founded: 1997 | Publisher Sakarya University |  
<http://www.saujs.sakarya.edu.tr/en/>

Title: Theoretical and Experimental Comparison of Micro-hardness and Bulk Modulus of Orthorhombic  $\text{YBa}_2\text{Cu}_3\text{-xZnxO}$  Superconductor Nanoparticles Manufactured using Sol-Gel Method

Authors: Elif AŞIKUZUN, Özgür ÖZTÜRK

Received: 2020-01-16 14:51:33

Accepted: 2020-06-20 17:02:42

Article Type: Research Article

Volume: 24

Issue: 5

Month: October

Year: 2020

Pages: 854-864

How to cite

Elif AŞIKUZUN, Özgür ÖZTÜRK; (2020), Theoretical and Experimental Comparison of Micro-hardness and Bulk Modulus of Orthorhombic  $\text{YBa}_2\text{Cu}_3\text{-xZnxO}$  Superconductor Nanoparticles Manufactured using Sol-Gel Method. Sakarya University Journal of Science, 24(5), 854-864, DOI: <https://doi.org/10.16984/saufenbilder.676028>

Access link

<http://www.saujs.sakarya.edu.tr/en/pub/issue/56422/676028>

New submission to SAUJS

<http://dergipark.org.tr/en/journal/1115/submission/step/manuscript/new>



## Theoretical and Experimental Comparison of Micro-hardness and Bulk Modulus of Orthorhombic $YBa_2Cu_{3-x}Zn_xO$ Superconductor Nanoparticles Manufactured using Sol-Gel Method

Elif AŞIKUZUN<sup>\*1</sup>, Özgür ÖZTÜRK<sup>2</sup>

### Abstract

In the present study, the sol-gel method was preferred for the production of superconductor materials since it is known that the sol-gel method is useful in producing nanoparticles. The Zn (Zinc) doped *YBCO*-123 superconductor samples ( $YBa_2Cu_{3-x}Zn_xO$ ) were produced. The main objective in the present study was to examine the effects of both of Zn doping and sol-gel method, which was chosen as the production method, on the structural, electrical, and mechanical properties of Y-123 superconductor materials. Especially, the effects of the nanoparticles and doping on the mechanical properties of materials were discussed over the bulk modulus. It was aimed to obtain information about the mechanical properties by comparing the bulk modules calculated theoretically and experimentally. Besides that, the XRD, SEM, and resistivity measurements were performed in order to characterize the structural and electrical properties.

**Keywords:** Sol-gel, vickers, bulk modulu, micro-hardness

### 1. INTRODUCTION

The mechanical behavior of the materials reflects the deformation or resistance of material against the force or load applied. Depending on the force applied to the material, two types of deformation occur; i) elastic (non-permanent change) and ii) plastic (permanent change). The elastic deformation refers to the change of distance between the atoms of material, on which the force is applied, without any separation between the adjacent atoms. When the applied force is

removed, then the object gains its previous form. If the stress created on the material by the force applied exceeds beyond the elasticity limit of the material, then the permanent deformation called plastic deformation occurs. In other words, the materials deform under the external forces. When the applied forces are removed, the deformation is called “elastic” (reversible) if the material gained its previous size and

\*Corresponding Author: [easikuzun@kastamonu.edu.tr](mailto:easikuzun@kastamonu.edu.tr)

<sup>1</sup>Kastamonu University, ORCID: <https://orcid.org/0000-0003-1850-7080>

<sup>2</sup>Kastamonu University, E-Mail: [oozturk@kastamonu.edu.tr](mailto:oozturk@kastamonu.edu.tr)

ORCID: <https://orcid.org/0000-0002-0391-5551>

shape, it is called “plastic” (permanent) if the previous form was not gained.

The hardness is defined as the material's resistance to the friction, scratch, cutting, and plastic deformation. The value obtained from the hardness measurements performed in the laboratories using special devices is the resistance of material against to the plastic deformation.

The most common and effective experiment carried out in order to determine the mechanical properties of the materials is the hardness measurement. The main reasons for this are that the procedure is simple and that it damages the sample less than the other procedures do. The other advantage is that the hardness of a material is directly proportionate to the other mechanical properties [1-4]. For instance; the tensile strength of steels is directly proportionate to the hardness. Thus, it is possible to have an idea about the strength of the material by measuring the hardness.

In the present study, the mechanical properties of the Zn doped YBCO-123 superconductor nanoparticles (YBa<sub>2</sub>Cu<sub>3-x</sub>Zn<sub>x</sub>O) which were produced using sol-gel method, are reported by making use of both experimental and theoretical data. The microhardness and bulk module values obtained experimentally were compared with the theoretically obtained results. Moreover, in order to determine the crystal structure and lattice parameters of the superconductors, the X-ray diffraction (XRD) measurements were performed, whereas ρ-T measurements were performed in order to examine the superconductor characteristics.

## 2. EXPERIMENTAL DETAILS

In the present study, the sol-gel method that is one of the methods most widely used for obtaining nano-sized samples was used. YBa<sub>2</sub>Cu<sub>3-x</sub>Zn<sub>x</sub>O samples were prepared by

using yttrium (III) acetate hydrate, barium acetate, copper (II) acetate, and zinc acetate dihydrate powders, as well as the acetic acid and methanol as solvents. 3 g powder mixtures (Y, Ba, Cu and Zn) were prepared for each sample and the zinc acetate dihydrate powder was added by 1%, 5%, 10%, 20%, and 50%. The solutions that were prepared were stirred using a heated magnetic stirrer for 8 hours with closed cover until obtaining a transparent solution. Then, the stirring process was continued for approx. 12 hours until the solution gelled. Then, the samples were dried in muffle furnace at 300° for 30 minutes. The powder samples were calcined for three times at 850° for 24 hours. The produced powder samples containing Zn were named *Zn*<sub>0.01</sub>, *Zn*<sub>0.05</sub>, *Zn*<sub>0.10</sub>, *Zn*<sub>0.20</sub>, and *Zn*<sub>0.50</sub>, whereas the undoped sample was named *Zn*<sub>0.00</sub>.

## 3. RESULTS

### 3.1. XRD and SEM Measurements

X-ray diffraction method was used to determine the crystal structures and lattice parameters of the materials. XRD measurements were performed by Bruker D8 Advance X-ray powder diffractometer using *CuK*<sub>α</sub> ( $\lambda = 1,541\text{Å}$ ) radiation in the range of  $3^{\circ} \leq 2\theta \leq 90^{\circ}$  at a scan speed of 4°/min. When XRD graph was examined, it was seen that the dominant phase in all samples was the Y-123 phase (Figure 1). There were no peaks of Zn ion doped instead of Cu ion. This result was shown that Zn ions entered into the YBCO structure [5, 6]. In addition, the ionic radius (0.73 Å) of the Cu (+2) ion was comparable with the ionic radius of the doped Zn (+2) ion (0.74 Å).

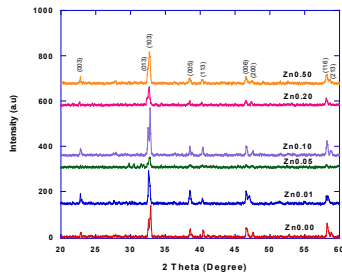


Figure 1 XRD patterns for all samples

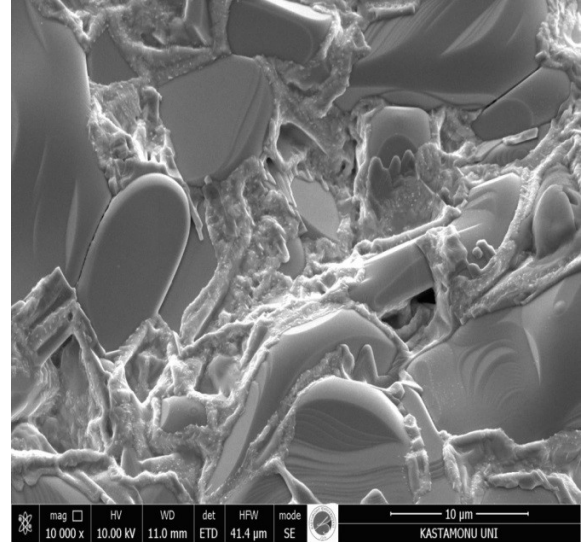
In the literature, the lattice constants of the Y-123 system which has orthorhombic symmetry ( $a \neq b \neq c$ ) are  $a = 3.82 \text{ \AA}$ ,  $b = 3.89 \text{ \AA}$  ve  $c = 11.7 \text{ \AA}$ . In this study, it was seen that the lattice parameters and crystal structure obtained for the Zn doped Y-123 system conformed with the literature (Table 1). In addition, grain sizes of the samples were calculated using the Warren-Scherrer equation [7]. As can be seen from Table 1, the Zn doping was decreased the grain size compared with the undoped sample.

Table 1  
 $a$ ,  $b$ ,  $c$  lattice parameters and grain size values of samples

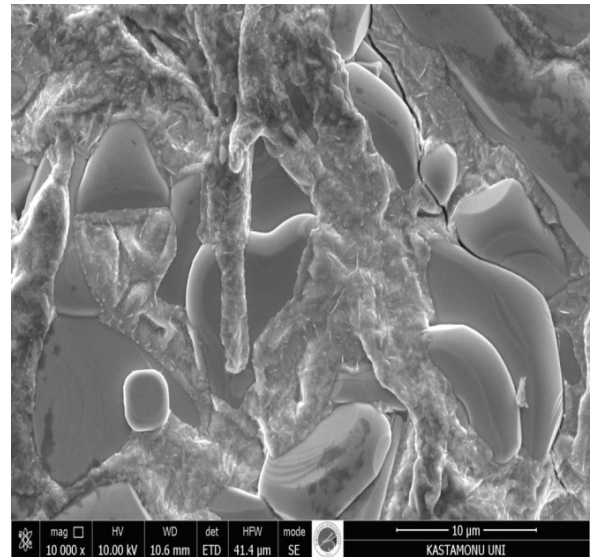
Samples	Lattice Parameters			Grain Size (nm)
	$a$ (Å)	$b$ (Å)	$c$ (Å)	
<b>Zn<sub>0.00</sub></b>	3.81	3.89	11.65	92.39
<b>Zn<sub>0.01</sub></b>	3.85	3.83	11.02	77.96
<b>Zn<sub>0.05</sub></b>	3.88	3.87	10.77	72.06
<b>Zn<sub>0.10</sub></b>	3.81	3.80	10.98	63.67
<b>Zn<sub>0.20</sub></b>	3.83	3.83	10.54	60.93
<b>Zn<sub>0.50</sub></b>	3.82	3.79	10.99	60.71

The surface morphology of the samples was examined by using FEI brand QUANTA FEG 250 model scanning electron microscopy (SEM). The surface images obtained at 10000 magnifications were given in Figure 2.

According to SEM results, we can say that grain size decreased and inter-particle pores increased with increasing the Zn doping.



a) Zn0.00



b) Zn0.05

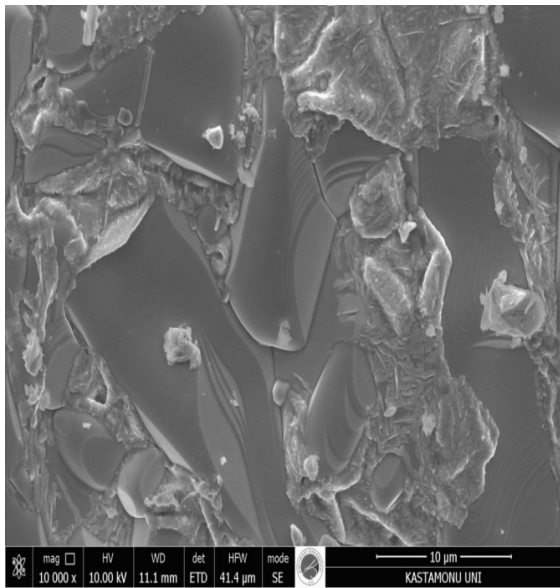
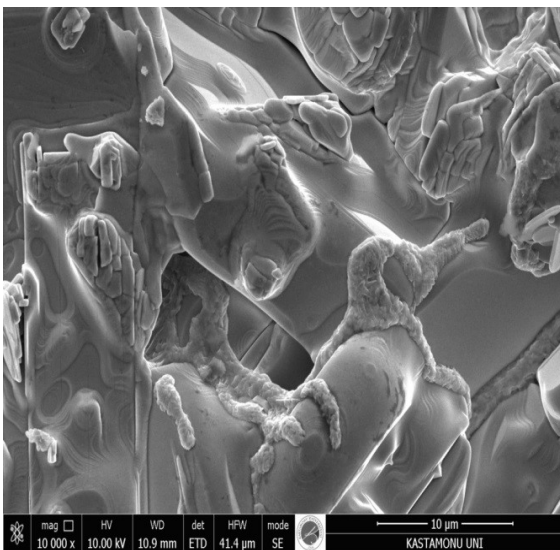
c) Zn<sub>0.10</sub>d) Zn<sub>0.20</sub>

Figure 2 SEM images for all samples

### 3.2. Resistivity Measurements

For electrical measurements, contacts were performed by a standard four-point method using a silver paste on the surface of samples. The He cooled closed-circuit cryostat system, the Lakeshore 336 temperature controller, the Keitley 2400 current source and the Keithley 2182 A Nanovoltmeter devices were used.

Above the onset transition temperatures ( $T_c^{onset}$ ) of the samples were determined as the transition temperature from normal state to superconducting state were shown metallic behavior (Fig. 3).  $T_c^{onset}$  were 89K, 84K, 75K, 56K and 54K for undoped, Zn<sub>0.01</sub>, Zn<sub>0.05</sub>, Zn<sub>0.10</sub> and Zn<sub>0.20</sub> samples, respectively. Zn<sub>0.50</sub> sample showed insulating behavior. Zn doping negatively affected to  $T_c^{onset}$ . However, the effect of nanoparticles on the electrical properties of materials was not determined.

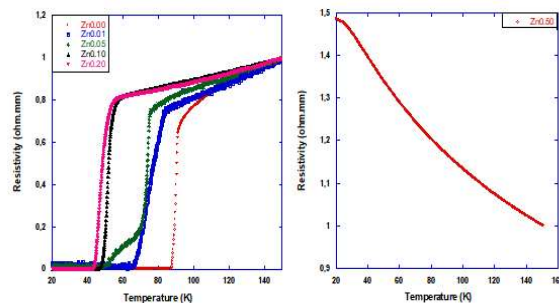


Figure 3 Normalized resistivity as a function of temperature curves for all samples

### 3.3. Microhardness measurements

The mechanical characterizations of samples were carried out using Shimadzu brand HMV-2 model digital static microhardness tester. The hardness is generally determined by measuring the resistance of material against a standard conic or spherical tip. The tip that is chosen appropriately leaves a trace on the material when it is pushed on the material under a constant load. In general, the hardness of the material is inversely proportional to the size of this trace [8-10]. The hardness measurements, which are performed in laboratories by using special devices, are classified based on the tip being used, the force being applied, the size of trace, and the method of measurement. The most widely used microhardness measurement methods are Brinell, Rockwell, Knoop, and Vickers methods.

In the present study, the Vickers microhardness measurement method, in which a diamond tip is used in order to prevent the negative consequences of the change of the geometrical shape of trace observed in Brinell experiment, was preferred. In the Vickers method, the pyramid stinging tip with 136° of apex angle between the counter-surfaces of the pyramid having square base is stung onto the sample for 10 seconds under force (F). Five different levels of force (0.245, 0.490, 0.980, 1.960, and 2.940 N) were applied to the superconductor samples during the procedures. After removing the load, two diagonal length of the trace ( $d_1$  and  $d_2$ ) on the material are measured using a microscope and the arithmetic mean ( $d$ ) is calculated. This procedure is repeated for minimum 10 times for each load and the mean value is calculated. Vickers hardness value is the proportion of load expressed in gram to the area of trace expressed in  $\mu\text{m}^2$ . Vickers microhardness value is calculated using the formula below,

$$H_V = 1854.4 \frac{F}{d^2} \quad (1)$$

The microhardness values obtained experimentally are presented in Table 2. Moreover, the diagram of the change in microhardness depending on the force applied ( $H_V$ -F) is presented in Figure 4. As seen in the figure, the microhardness values increased in parallel with the load applied. This behavior is defined as RISE (Reverse Indentation Size Effect) in the literature. These materials exhibit only the plastic deformation. No elastic deformation is observed or it is at much lower levels when compared to the plastic deformation. Furthermore, as it can be seen in Figure 3, the hardness values did not change when the loads higher than 1N were applied. In and after this region that is called the saturation region, there would be no significant change in the hardness value even if the load applied

is increased [11-14]. While calculating the microhardness values, the bulk modulus of the material were calculated by using Equation (2).

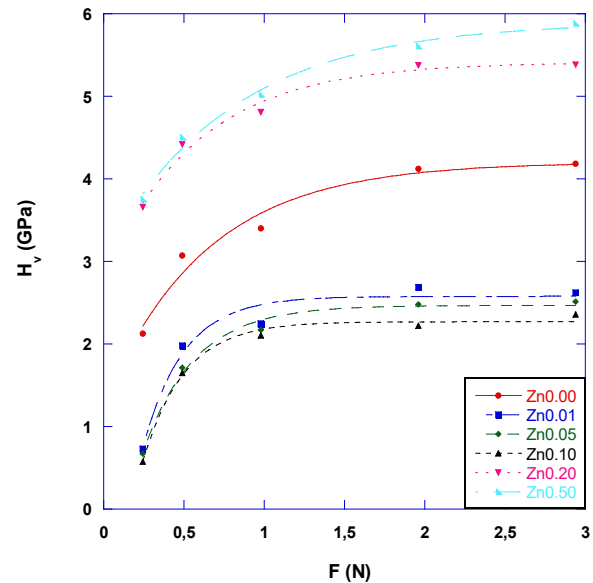


Figure 4 Vickers microindention hardness variation as a function of indentation test load for all samples

$$B = 81.9635 H_V \quad (2)$$

The bulk module is an elastic characteristic that defines the decrease in a material exposed to a applied force. The results obtained are presented in Table 2. As it can be seen in the table, the microhardness value of the material did not change in parallel with the Zn doping when compared to the undoped sample. The microhardness values decreased in  $Zn_{0.01}$ ,  $Zn_{0.05}$ , and  $Zn_{0.10}$  samples and decreased in  $Zn_{0.20}$  and  $Zn_{0.50}$  samples. The decrease observed here is related with the status of impurity phases and irregularity. These factors lead the strong bonds to weaken and, thus, the microhardness to decrease. Moreover, the decrease in value of  $H_V$  causes increase in resistivity between the particles,

reduction in the interparticular transmission surface, and weakening in the borders of particles. Here, the material behavior did not

change but the microhardness values were observed to change in parallel with the Zn doping.

Table 2

The experimental values of  $H_v$  and  $B$  weakening in the borders of particles.

Samples	F (N)	Exp. $H_v$ (GPa)	Exp. $B$ (GPa)
<b>Zn<sub>0.00</sub></b>	0.245	2.126	174.27
	0.490	3.073	251.92
	0.980	3.401	278.78
	1.960	4.121	337.84
	2.940	4.186	343.11
<b>Zn<sub>0.01</sub></b>	0.245	0.728	59.72
	0.490	1.979	162.23
	0.980	2.245	184.08
	1.960	2.687	220.30
	2.940	2.621	214.87
<b>Zn<sub>0.05</sub></b>	0.245	0.672	55.10
	0.490	1.715	140.56
	0.980	2.173	178.14
	1.960	2.478	203.12
	2.940	2.513	205.99
<b>Zn<sub>0.10</sub></b>	0.245	0.576	47.21
	0.490	1.651	135.32
	0.980	2.105	172.54
	1.960	2.224	182.28
	2.940	2.360	193.43
<b>Zn<sub>0.20</sub></b>	0.245	3.658	299.85
	0.490	4.416	362.02
	0.980	4.808	394.10
	1.960	5.377	440.72
	2.940	5.385	441.38
<b>Zn<sub>0.50</sub></b>	0.245	3.753	307.64
	0.490	4.503	369.09
	0.980	5.019	411.44
	1.960	5.608	459.69
	2.940	5.882	482.16

In order to be able to compare the experimental results that we obtained to the theoretical results, an empirical approach was developed for the bulk module [15]. In this approach, it is possible to obtain a projectable

value in examining the bulk modules of all the compounds consisting of elements between I and VII [15]. Given the results, there is an approx. scale for these materials.

$$B=550d^{-3} \quad (3)$$

The  $d$  here refers to the bond length of the crystal structure. The doping applied to the materials may cause local planar defects on the samples. These defects cause extra reflections arising from  $n$  different planes differing from the XRD patterns. These changes create changes in the mean length of bond.

As known, different crystal structures have different lengths of bond. The lengths of these bonds vary depending on the lattice parameters of the crystal. The YBCO superconducting materials have body-centered orthorhombic crystal structure. Some of the important characteristics of orthorhombic structure are provided below;

Lattice parameters  $a \neq b \neq c$

Bond angles  $\alpha = \beta = \gamma = 90$

$$\text{Bond length } d = \sqrt{\frac{a^2}{9} + c^2 \left(\frac{1}{4} - u\right)^2} \quad (4)$$

$u$  is related with  $c/a$ .

$$u = 0.24 \sqrt{1 - a^2/c^2} \quad (5)$$

Using the theoretical B values calculated with Equation 3, the theoretical microhardness values were calculated (Eqn.2). All of the calculated values are presented in Table 3. The calculated values are different from the experimental values. This can be explained with the difference of samples' porosity from the estimated values. Moreover, the theoretically calculated B value depends on the bond length. The bond length depends on the lattice parameters. Since the crystal structure of examined materials did not change with the doping, no significant change was observed in the lattice parameters and consequently the bond lengths. The crystal structures of samples with and without

doping are body-centered orthorhombic. This crystal structure is also seen in data cards obtained from the XRD measurement. Besides that, the bulk module values obtained experimentally are calculated with a force applied on the surface of sample. The possible accumulation at the particle borders or porosity changing with the doping directly affects the hardness measurements. Detecting this difference is almost impossible in theoretical calculations. Thus, the difference between the theoretically calculated values and the experimentally obtained ones can be explained.

Moreover, in the literature, there are the mathematical models used in microhardness analysis. As specified in previous studies, these are Meyer's law, proportional sample resistance (PSR) model, elastic/plastic deformation (EPD) model, Hays-Kendall (HK) approach, and indentation-induced cracking (IIC) model [16, 17]. The main purpose of applying these models is to achieve the theoretical model that is closest to the experimentally obtained microhardness values. Among these models, the model that is most appropriate for the materials exhibiting RISE behavior is generally reported to be the IIC model [18, 19]. In the present study, only the IIC model is explained in supporting the theoretical calculations.

• *Mechanic Analysis according to the Indentation Induced Cracking (IIC) Model*

This model is a model developed to explain RISE behavior [20]. It is about the reaction of the sample at maximum depth against the load applied to the surface of the material. There are different reasons of the reaction of the material. The most important of these are the shift of the tip or sample on the interface, the elastic and plastic deformation or the cracks formed in the sample. According to Li and Bradt, the cracks cause to exhibiting RISE behavior of the sample [18]. The cracks prevent to exhibiting elastic deformation of

the sample and the material only shows plastic deformation. That is, elastic recovery is either absent or very small in samples exhibiting RISE behavior. The theoretical hardness value calculated by this model is given by Eqn. (7).

$$H_v = K(F^{5/3}/d^3)^m \quad (7)$$

The values  $K$  and  $m$  obtained from the  $\ln H_v - \ln(F^{5/3}/d^3)$  graph are load-

independent constants (Figure 5). If  $m$  value obtained from the slope of the graph is greater than 0.6, the material exhibits RISE behavior. The microhardness values calculated according to the model were given in Table 4. As seen clearly from the table, the microhardness values were quite close to the values in the plateau region. This result is also in agreement with the theoretical results obtained using Eqn. (6).

Table 3  
Calculated theoretical values

Samples	Bond Length	u	Theoretical B	Theoretical H	Experimental B (Average)	Experimental H (Average)
<b>Zn<sub>0.00</sub></b>	1.274	0.285	265.72	3.242	277.18	3.381
<b>Zn<sub>0.01</sub></b>	1.297	0.290	251.84	3.072	137.29	2.052
<b>Zn<sub>0.05</sub></b>	1.312	0.293	243.28	2.968	130.54	1.910
<b>Zn<sub>0.10</sub></b>	1.282	0.290	260.49	3.178	120.32	1.783
<b>Zn<sub>0.20</sub></b>	1.296	0.294	252.10	3.075	370.61	4.728
<b>Zn<sub>0.50</sub></b>	1.286	0.290	258.29	3.151	394.90	4.953

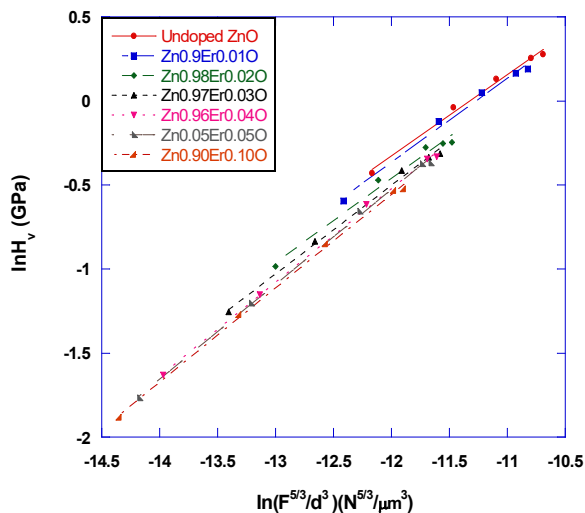


Figure 5 Variation of  $\ln(H_v)$  with  $\ln(F^{5/3}/d^3)$  according to IIC model for all samples

Table 4  
Experimental microhardness values

Samples	m	ln K	H <sub>IIC</sub>
<b>Zn<sub>0.00</sub></b>	0.47	5.72	3.581
<b>Zn<sub>0.01</sub></b>	0.56	6.43	1.547
<b>Zn<sub>0.05</sub></b>	0.56	6.42	2.944
<b>Zn<sub>0.10</sub></b>	0.56	6.49	3.732
<b>Zn<sub>0.20</sub></b>	0.39	5.08	4.883
<b>Zn<sub>0.50</sub></b>	0.41	5.25	4.981

#### 4. CONCLUSIONS

In the present study, the Zn doped YBCO-based high-temperature superconducting samples were produced using sol-gel method and their structural, electrical, and mechanical properties were analyzed. The

superconductivity characteristics of the samples were determined by using dc resistivity, the mechanical properties were determined using Vickers microhardness, and the surface morphology, crystal structure characteristics, and lattice parameters were determined using *XRD* and *SEM* measurements. The results obtained are summarized below.

- In diffraction patterns obtained from XRD analyses, no remarkable second phase or peak related with Zn ion was observed. All of the phases obtained here are the characteristic phases of YBCO.
- It can be seen that the *a* lattice parameters of the samples increased up to Zn<sub>0.05</sub> and then decreased. *c* lattice parameter, however, decreased until Zn<sub>0.05</sub> and then showed increase. This finding indicates that the doping ratio of 0.05 is a threshold and the structure changed in all the doping ratios beyond this level.
- According to SEM results, we can say that grain size decreased and inter-particle pores increased with increasing the Zn doping.
- It can be said that room temperature resistance increased with increasing Zn doping using R-T measurements.
- The microhardness values increased with increasing the applied load on the surface. That is, the material exhibited RISE behavior.
- The microhardness results were experimentally and theoretically calculated. When the obtained results were compared, it was determined that the theoretical values are lower. This difference can be explained with the difference of samples' porosity from the estimations and the result that the crystal structure did not change with the Zn doping.

### ***Acknowledgements***

We thank the Kastamonu University Research and Application Center and Kastamonu University Scientific Research Projects Coordination Department for the supports.

### ***Funding***

This study was supported by the Kastamonu University Scientific Research Projects Coordination Department under the Grant No. KÜ-BAP01/2016-21.

### ***The Declaration of Conflict of Interest/ Common Interest***

No conflict of interest or common interest has been declared by the authors.

### ***Authors' Contribution***

All authors of the paper contributed actively to the parts of study such as experiments, analysis, writing and submission of article.

### ***The Declaration of Ethics Committee Approval***

The authors declare that this document does not require an ethics committee approval or any special permission.

### ***The Declaration of Research and Publication Ethics***

The authors of the paper declare that they comply with the scientific, ethical and quotation rules of SAUJS in all processes of the paper and that they do not make any falsification on the data collected. In addition, they declare that Sakarya University Journal of Science and its editorial board have no responsibility for any ethical violations that may be encountered, and that this study has not been evaluated in any academic publication environment other than Sakarya University Journal of Science.

## REFERENCES

- [1] R.L. Smith and G.E. Sandland, "An Accurate Method of Determining the Hardness of Metals, with Particular Reference to Those of a High Degree of Hardness," *Proceedings of the Institution of Mechanical Engineers*, 1, pp. 623-641, 1922.
- [2] S.M. Khalil, "Enhancement of superconducting and mechanical properties in BSCCO with Pb additions," *J. Phys. and Chem. Solids*, 62, pp. 457-466, 2001.
- [3] E. Asikuzun, O. Ozturk, H.A. Cetinkara, G. Yildirim, A. Varilci, M. Yilmazlar, and C. Terzioglu, "Vickers hardness measurements and some physical properties of Pr<sub>2</sub>O<sub>3</sub> doped Bi-2212 superconductors," *J. Mat. Sci. Mater. in Elect.*, 23, pp. 1001-1010, 2012.
- [4] S.M. Khalil, "Role of rare-earth Ba<sup>2+</sup> doping in governing the superconducting and mechanical characteristics of Bi-Sr-Ca-Cu-O," *Smart Mater. and Structure*, 14, 804, 2005.
- [5] H. Koralay, O. Hicyilmaz, S. Cavdar, E. Asikuzun, A.T. Tasci, and O. Ozturk, "Effect of Zn content on microstructure and mechanical performance in Bi<sub>1.8</sub>Sr<sub>2</sub>Ca<sub>2</sub>Cu<sub>3.22-x</sub>Zn<sub>x</sub>O<sub>10+δ</sub> glass ceramic," *J. Mat. Sci. Mater. in Elect.* 25, pp. 3116-3126, 2014.
- [6] H. Koralay, O. Hicyilmaz, S. Cavdar, E. Asikuzun, A.T. Tasci, and O. Ozturk, "Effect of Zn content on microstructure and mechanical performance in Bi<sub>1.8</sub>Sr<sub>2</sub>Ca<sub>2</sub>Cu<sub>3.22-x</sub>Zn<sub>x</sub>O<sub>10+δ</sub> glass ceramic," *Journal of Materials Science: Materials in Electronics*, 25, pp. 3116-3126, 2014.
- [7] E. Asikuzun, A. Donmez, L. Arda, O. Cakiroglu, O. Ozturk, D. Akcan, and C. Terzioglu, "Structural and mechanical properties of (Co/Mg) co-doped nano ZnO," *Ceramics International*, 41, pp. 6326-6334, 2015.
- [8] U. Kölemen, O. Uzun, M. Yilmazlar, N. Güçlü, and E. Yanmaz, "Hardness and microstructural analysis of Bi<sub>1.6</sub>Pb<sub>0.4</sub>Sr<sub>2</sub>Ca<sub>2-x</sub>Sm<sub>x</sub>Cu<sub>3</sub>O<sub>y</sub> polycrystalline superconductors," *J. Alloys and Compounds*, 415, pp. 300-306, 2006.
- [9] R. Awad, A.A. Aly, M. Kamal, and M. Anas, "Mechanical Properties of (Cu<sub>0.5</sub>Tl<sub>0.5</sub>)-1223 Substituted by Pr," *J. Supercond. and Novel Magn.*, 24, pp. 1947-1956, 2011.
- [10] K. Sangwal, "On the reverse indentation size effect and microhardness measurement of solids," *Mater. Chem. and Phys.*, 63, pp. 145-152, 2000.
- [11] L. Arda, O. Ozturk, E. Asikuzun, and S. Ataoglu, "Structural and mechanical properties of transition metals doped ZnMgO nanoparticles," *Powder Technology*, 235, pp. 479-484, 2013.
- [12] A.A. Elmustafa and D.S. Stone, "Nanoindentation and the indentation size effect: Kinetics of deformation and strain gradient plasticity," *J. Mech. and Phy. Solids*, 51, pp. 357-381, 2003.
- [13] O. Ozturk, E. Asikuzun, and G. Yildirim, "The role of Lu doping on microstructural and superconducting properties of Bi<sub>2</sub>Sr<sub>2</sub>CaLu<sub>x</sub>Cu<sub>2</sub>O<sub>y</sub> superconducting system," *J. Mat. Sci. Mater. in Elect.*, 24, pp. 1274-1281, 2013.
- [14] H. Koralay, A. Arslan, S. Cavdar, O. Ozturk, E. Asikuzun, A. Gunen, and A.T. Tasci, "Structural and Mechanical Characterizations of Bi<sub>1.75</sub>Pb<sub>0.25</sub>Sr<sub>2</sub>Ca<sub>2</sub>Cu<sub>3-x</sub>Sn<sub>x</sub>O<sub>10+δ</sub> Superconductor Ceramics Using Vickers Microhardness Test," *J. Mat. Sci. Mater. in Elect.*, 24, pp. 4270-4278, 2013.
- [15] L. Martin Cohen, "Calculation of bulk moduli of diamond and zinc-blende solids," *Phys. Rev. B*, 32, pp. 7988-7991, 1985.

- [16] O. Ozturk, H.A. Cetinkara, E. Asikuzun, M. Akdogan, M. Yilmazlar, and C. Terzioglu, "Investigation of mechanical and superconducting properties of iron diffusion-doped Bi-2223 superconductors," *J. Mat. Sci. Mater.in Elect.*, 22, pp. 1501-1508, 2011.
- [17] M. Tosun, S. Ataoglu, L. Arda, O. Ozturk, E. Asikuzun, D. Akcan, and O. Cakiroglu, "Structural and mechanical properties of ZnMgO nanoparticles," *J. Mater. Sci. Eng. A.*, 590, pp. 416-422, 2014.
- [18] E. Asikuzun, O. Ozturk, L. Arda, D. Akcan, S.D. Senol, and C. Terzioglu, "Preparation, structural and micromechanical properties of (Al/Mg) co-doped ZnO nanoparticles by sol-gel process," *J. Mat. Sci.: in Elect.*, 26, pp. 8147-8159, 2015.
- [19] O. Ozturk, E. Asikuzun, S. Kaya, M. Erdem, S. Safran, A. Kilic, and C. Terzioglu, "Ac Susceptibility Measurements and Mechanical Performance of Bulk MgB<sub>2</sub>," *J. Supercond. Nov. Magn.*, 28, pp. 1943-1952, 2015.
- [20] H. Li and R.C. Bradt, "The microhardness indentation load/size effect in rutile and cassiterite single crystals," *J. Mater. Sci.*, 28, pp. 917-926, 1993.